

Articles

Exploring the Active Site of *Trypanosoma brucei* Phosphofructokinase by Inhibition Studies: Specific Irreversible Inhibition[†]

Samantha Claustre,[‡] Colette Denier,[‡] Faouzi Lakhdar-Ghazal,[‡] Andrée Lougare,[‡] Claudia Lopez,[§]
Nathalie Chevalier,[§] Paul A. M. Michels,[§] Jacques Périé,[‡] and Michèle Willson^{*,‡}

Laboratoire Synthèse et Physico Chimie de Molécules d'Intérêt Biologique UMR–CNRS 5068, Université Paul Sabatier,
118 route de Narbonne, 31062 Toulouse Cedex, France, and Research Unit for Tropical Diseases, Christian de Duve Institute
of Cellular Pathology and Laboratory of Biochemistry, Université Catholique de Louvain, Brussels, Belgium

Received January 25, 2002; Revised Manuscript Received May 8, 2002

ABSTRACT: This work deals with the phosphofructokinase enzyme (PFK) of the parasite *Trypanosoma brucei*. Inhibitors which are analogues of fructose-6-phosphate (F6P) derived from 2,5-anhydromannitol and therefore blocked in a closed conformation, both nonphosphorylated and phosphorylated, were designed. They provided information on this class of ATP-dependent PFK (structurally more similar to PPi-dependent PFKs revealing (i) an ordered mechanism, ATP binding first, inducing an essential conformational change to increase the affinity for F6P, and (ii) a rather hydrophobic environment at the ATP binding site. Nonphosphorylated mannitol derivatives bind at both the ATP and F6P binding sites, whereas the phosphorylated derivatives only bind at the ATP binding site. The inhibitors bearing an aromatic ring substituted at the meta position indicate a polar interaction with lysine 227, which is specific to *T. brucei* PFK and is replaced by a glycine in human PFK. This lysine can be irreversibly bound, leading to inhibition when an electrophilic carbon atom is β to the meta position on the ring. This lysine was identified by site-directed mutagenesis. This first example of a specific irreversible inactivation of *T. brucei* PFK offers an opportunity to develop biologically active compounds against the sleeping sickness, the causative agent of which is the trypanosome.

Despite the abundance of previous studies, glucose metabolism in Trypanosomatidae continues to be the source of new research in terms of both fundamental aspects and inhibitor design (1, 2). The compartmentation of the glycolytic enzymes (3) is considered to be responsible for their specific structural and kinetic features and, in parallel, for the unique mechanism by which the concentration of hexose

phosphates and the ATP/ADP ratio are controlled (4, 5). Moreover, for parasites such as *Trypanosoma brucei*, the causative agent of sleeping sickness in Africa, glycolysis is the sole source of ATP (6); the design of new inhibitors of this process therefore represents a strategic opportunity for the development of new trypanocidal drugs, as long as the inhibition brought about is specific for the parasite enzymes (7, 8).

In *T. brucei*, regulation of the activity of the glycosomal hexokinase (HK)¹ and phosphofructokinase (PFK) seems to be relatively unimportant (9–11); in contrast, the cytosolic pyruvate kinase (PyK) have been reported to be the only major regulated enzyme in the glycolytic pathway of these

[†] This research was financially supported by the European Union (Contracts IC18-CT 960079 and IC180-CT 970220) and by la Société de Secours des Amis de la Science, which are both fully acknowledged.

* Corresponding author. E-mail: willson@chimie.ups-tlse.fr. Fax: (33) 5 61 55 60 11.

[‡] UMR-CNRS 5068, Université Paul Sabatier.

[§] Université Catholique de Louvain.

parasites (12, 13), and the allosteric activators identified to date are fructose-2,6-diphosphate (F2,6P) and, to some extent, fructose-1,6-diphosphate (F1,6P). *T. brucei* PFK (EC 2.7.1.11) (9–11, 14), which transforms fructose-6-phosphate (F6P) into F1,6P by ATP–Mg, has been selected as a target for the action of trypanocides because it is responsible for the formation of one of the PyK effectors. Cloning of its gene and comparison of the predicted amino acid sequence with PFK sequences from different organisms indicated that the glycosomal ATP-dependent PFK of *T. brucei* is more similar to pyrophosphate PP_i-dependent PFKs than to other ATP-dependent PFKs (15). One of the consequences is the occurrence of significant differences at its active site compared to other ATP-dependent PFKs, including the various human isoenzymes.

Owing to these different reasons, we designed inhibitors for *T. brucei* PFK. Because of the lack of a crystal structure for trypanosomatid PFK or a sufficiently similar enzyme that would permit the construction of a reliable structure model, we designed the inhibitors according to the following strategy: (1) exploration of the active site of this enzyme with compounds close in structure to the substrate, F6P, in order to determine the kind of inhibitor that could be proposed; so far, no PFK-specific active-site inhibitors have been described in the literature; (2) exploration of the possibility of covalently linking one of these inhibitors to the protein, because irreversible inhibitors are expected to be more efficient in blocking the glycolytic flux (1); and (3) identification of any residues involved in the covalent binding by site-directed mutagenesis.

In addition, the nature of ligand binding was further studied by investigating the effect on conformational changes of the enzyme by fluorescence spectroscopy and circular dichroism. The strategy proposed for inhibitor development was successfully pursued by using cyclic analogues of F6P, phosphorylated-2,5-anhydromannitol derivatives.

MATERIALS AND METHODS

Source of Enzymes, Substrates, and Cofactors. Fructose-6-phosphate, ATP, NADH, phosphoenol pyruvate, the linking enzymes pyruvate kinase (PyK), lactate dehydrogenase (LDH), aldolase, triosephosphate isomerase (TIM), and glycerol-3-phosphate dehydrogenase (GPDH) were purchased from Sigma-Aldrich Chemicals Co. (St. Louis, MO) and Roche (Mannheim, Germany).

Expression and Purification of Recombinant PFK. To produce recombinant *T. brucei* PFK, the complete gene (15) was amplified and ligated in vector pET15b (Novagen, Darmstadt, Germany) in such a way that an open-reading frame was created for a fusion protein of PFK with an N-terminal extension of 20 amino acids, including a stretch of six histidine residues. The recombinant plasmid was introduced in *Escherichia coli* BL21(DE3)pLysS cells also

containing a plasmid coding for chaperonin GroE and kanamycin resistance. The coexpression of the chaperonin appeared to result in a somewhat higher yield of soluble PFK. Bacteria were grown as 50 mL cultures in LB medium supplemented with 100 µg/mL ampicillin, 25 µg/mL chloramphenicol, and 50 µg/mL kanamycin at 30 °C with vigorous shaking. A total of 0.4 mM isopropyl thio-β-D-galactoside was added at an OD_{600 nm} of 0.5 to induce expression of PFK and growth was continued for another 15 h. The cells were harvested by centrifugation and resuspended in 20 mL of lysis buffer containing 50 mM triethanolamine/HCl (pH 8.0), 50 mM KCl, 1 mM potassium phosphate, 5 mM MgCl₂, 10% glycerol, 0.3 mM fructose-6-phosphate, 1 mM glucose-6-phosphate, and the protease inhibitors E64, leupeptin, and pepstatin, each at a concentration of 1 µM. The cells were disrupted by two passages through a SLM-Aminco French Press cell at 90 MPa. Nucleic acids were removed by incubation with 200 U of benzonase (Merck, Whitehouse Station, NJ) for 15 min at 37 °C and protamine sulfate (0.5 mg/mL) for 15 min at room temperature followed by centrifugation for 10 min at 12 000g. The supernatant was applied onto the metal chelating resin (2 mL Talon resin; Clontech), exploiting the enzyme's histidine tag for its purification. The charged resin was washed 4 times with 5 mL of lysis buffer containing 5 mM imidazole; the PFK was eluted with 10 × 1 mL of lysis buffer supplemented with 100 mM imidazole. One-milliliter fractions were collected to measure enzyme activity and to determine the protein profile by SDS–PAGE. The PFK samples thus obtained were more than 95% pure as assessed by SDS/PAGE.

Site-Directed Mutagenesis of *T. brucei* PFK. Codon AAG of residue Lys226 was changed into the glycine codon GGG by using the PCR method described by Mikaelian and Sergeant (16). This involved the amplification of the 5' half of the PFK gene. The PCR product was subsequently used to replace the corresponding segment in the wild-type gene. Another mutant, where the codon TAC of residue Tyr139 was replaced by TTC for phenylalanine, was made by using Stratagene's Quick Change site-directed mutagenesis kit. The presence of the mutations and the absence of any other changes in the gene were ascertained by sequencing. The mutated plasmids were introduced into *E. coli* BL21(DE3)-pLysS cells. The mutant PFKs were expressed and purified as described for the wild-type enzyme but using slightly modified growth conditions; the LB medium was supplemented with 1 M sorbitol and 2.5 mM betaine to cause osmotic stress resulting in a larger fraction of soluble recombinant protein (17).

Synthesis of Inhibitors. The pure compounds were identified by spectrometric analysis at the Institute of Molecular Chemistry Paul Sabatier (ICMPS–IR1744): IR spectra were recorded on a PerkinElmer FTIR 1610 spectrometer, ¹H and ¹³C NMR spectra were run on a Bruker 250 MHz FT apparatus, and mass spectra were determined on a Nemaq R10-10.

The synthesis of 2,5-anhydromannitol used in this study has been described elsewhere (18). The reaction of phosphorylation on the primary alcohol group was attempted without protection of secondary alcohol and amino groups using two different phosphorylating reagents: (i) for nitro derivatives 8–10, we used 2-(*N,N*-dialkylamino)-4-nitrophenyl phosphate (19), which directly yielded the phosphoric

¹ Abbreviations: ADP, adenosine diphosphate; AMP, adenosine monophosphate; ATP, adenosine triphosphate; EDTA, ethylenediaminetetraacetic acid; F26P, fructose-2,6-bisphosphate; F6P, fructose-6-phosphate; GPDH, glycerol-3-phosphate dehydrogenase; HK, hexokinase; LDH, lactate dehydrogenase; NAD⁺, nicotinamide adenine dinucleotide (oxidized form); NADH, nicotinamide adenine dinucleotide (reduced form); NMR, nuclear magnetic resonance; PEP, phosphoenol pyruvate; PFK, phosphofructokinase; PyK, pyruvate kinases; TIM, triosephosphate isomerase.

monoester; and (ii) for compounds **11–13**, dibenzylpyridinium iodophosphate was converted into the dihydrogenophosphate compound, after hydrogenolysis of the corresponding dibenzyl ester (20).

(i) *Synthesis of Nitro Derivatives 8–10*. 2,5-Anhydro-1-deoxy-1-(*m*-nitrophenylamino)-D-mannitol-6-disodiumphosphate, **8** (yield 93%), ^{13}C NMR (D_2O , δ): 152.05 (C-7), 151.95 (C-9), 132.17 (C-11), 121.19 (C-12), 113.78 (C-10), 106.99 (C-8), 84.03 ($^3J_{\text{C-P}} = 6.59$ Hz, C-5), 83.20 (C-2), 80.88 (C-3), 78.81 (C-4), 68.15 ($^2J_{\text{C-P}} = 6.64$ Hz, C-6), 47.13 (C-1); ^{31}P NMR (D_2O , δ): -3.56 ; MS (negative FAB, glycerol) m/z : 385 [$\text{M} - \text{Na}^+$] $^-$, 363 [$\text{M} - 2\text{Na}^+ + \text{H}$] $^-$.

2,5-Anhydro-1-deoxy-1-(*m*-dinitrophenylamino)-D-mannitol-6-biscyclohexylammonium phosphate, **9** (yield 75%), ^1H NMR (D_2O , δ): 7.27–7.00 (m, 5H, H-8, H-12), 4.08–3.80 (m, 4H, H-2, H-3, H-4, H-5), 3.55–2.90 (m, 4H, H-1a, H-1b, H-6a, H-6b); ^{13}C NMR (D_2O , δ): 151.99 (C-7), 150.75 (C-9, C-11), 112.21 (C-8, C-12), 105.52 (C-10), 83.79 ($^3J_{\text{C-P}} = 6.61$ Hz, C-5), 81.29 (C-2), 79.57 (C-3), 77.80 (C-4), 68.73 ($^2J_{\text{C-P}} = 6.50$ Hz, C-6), 51.58 (CH cyclohexyl), 47.13 (C-1), 32.04, 25.95, 25.43 (CH_2 cyclohexyl); ^{31}P NMR (D_2O , δ): -3.28 ; MS (FAB < 0 , glycerol) m/z : 507 [$\text{M} - \text{C}_6\text{H}_{14}\text{N}^+$] $^-$.

2,5-Anhydro-1-deoxy-1-(*p*-fluoro-*m*-nitrophenylamino)-D-mannitol-6-disodiumphosphate, **10** (yield 85%), ^1H NMR (D_2O , δ): 7.41 (m, 1H, H-8), 7.14 (d, 1H, $J_{10,11} = J_{11,12} = 8.8$ Hz, H-11), 7.06 (m, 1H, H-12), 4.23 (m, 1H, H-5), 4.16 (m, 1H, H-4), 4.01 (m, 1H, H-3), 3.85 (m, 1H, H-2), 3.72–3.63 (m, 2H, H-6a, H-6b), 3.41–3.30 (m, 2H, H-1a, H-1b); ^{13}C NMR (D_2O , δ): 149.03 (C-7), 147.70 (C-10), 139.43 (C-9), 124.49 (C-12), 121.46 (C-11), 111.62 (C-8), 85.34 ($^3J_{\text{C-P}} = 7.23$ Hz, C-5), 83.98 (C-2), 80.87 (C-3), 79.34 (C-4), 66.71 ($^2J_{\text{C-P}} = 5.62$ Hz, C-6), 48.33 (C-1); ^{31}P NMR (D_2O , δ): $+3.25$; MS (negative FAB, glycerol) m/z : 403 [$\text{M} - \text{Na}^+$] $^-$.

(ii) *Synthesis of Compounds 11–13*. 2,5-Anhydro-1-deoxy-1-(*m*-carboxyphenylamino)-D-mannitol-6-phosphate, **11** (yield 80%). This synthesis was carried out using product **4** bearing the protected carboxyl function (the benzyl carboxyl ester) which was removed by a hydrogenolysis step. ^1H NMR (CD_3OD , δ): 7.45–6.88 (m, 4H, H-8 to H-12), 4.05–3.79 (m, 4H, H-3, H-2, H-4, H-5), 3.75–3.50 (m, 4H, H-1a, H-1b, H-6a, H-6b); ^{13}C NMR (CD_3OD , δ): 172.5 (C-13), 151.55 (C-7), 133.95 (C-9), 132.03 (C-11), 121.0 (C-12), 119.3 (C-10), 115.81 (C-8), 84.82 ($^3J_{\text{C-P}} = 7.2$ Hz, C-5), 83.85 (C-2), 81.05 (C-3), 79.10 (C-4), 66.15 ($^2J_{\text{C-P}} = 5.8$ Hz, C-6), 47.66 (C-1); ^{31}P NMR (D_2O , δ): $+2.96$; MS (negative FAB, glycerol) m/z : 362 [$\text{M} - \text{H}^+$] $^-$.

2,5-Anhydro-1-deoxy-1-(*m*-chlorophenylamino)-D-mannitol-6-disodiumphosphate, **12** (yield 80%) ^1H NMR (D_2O , δ): 7.51 (m, 1H, H-11), 7.15 (t, 1H, H-8), 6.81 (dd, 2H, H-10, H-12), 4.27–3.95 (m, 6H, H-2, H-6), 3.35 (m, 2H, H-1a, H-1b); ^{13}C NMR (D_2O , δ): 148.41 (C-7), 136.11 (C-9), 131.70 (C-11), 120.74 (C-10), 115.99 (C-8), 114.85 (C-12), 84.49 ($^3J_{\text{C-P}} = 6.62$ Hz, C-5), 83.69 (C-2), 79.92 (C-3), 78.67 (C-4), 67.20 ($^2J_{\text{C-P}} = 5.2$ Hz, C-6), 55.28 (C-1); ^{31}P NMR (D_2O , δ): $+0.84$; MS (negative FAB, glycerol) m/z : 352 [$\text{M} - \text{H}$] $^-$.

2,5-Anhydro-1-deoxy-1-phenylamino-D-mannitol-6-biscyclohexylammoniumphosphate, **13** (yield 48%), ^1H NMR (CD_3OD , δ): 7.27–7.00 (m, 5H, H-8 to H-12), 4.08 (m, 3H, H-3, H-4, H-5), 3.83 (m, 1H, H-2), 3.55–2.90 (m, 6H,

H-1a, H-1b, H-6a, H-6b, CH cyclohexyl), 2.05–1.23 (m, 20H, CH_2 cyclohexyl); ^{13}C NMR (CD_3OD , δ): 154.46 (C-7), 130.31 (C-8, C-12), 124.36 (C-9, C-11), 121.46 (C-10), 84.68 ($^3J_{\text{C-P}} = 7.35$ Hz, C-5), 80.93 (C-2), 80.79 (C-3), 78.66 (C-4), 67.05 ($^2J_{\text{C-P}} = 7.45$ Hz, C-6), 58.55 (CH cyclohexyl), 44.32 (C-1), 30.88, 26.28, 25.64 (CH_2 cyclohexyl); ^{31}P NMR (CD_3OD , δ): -3.11 ; MS (negative FAB, glycerol) m/z : 417 [$\text{M} - \text{C}_6\text{H}_{14}\text{N}^+$] $^-$.

(iii) *Synthesis of 2,5-Anhydro-1-deoxy-1-(*m*-isothiocyanophenylamino)-D-mannitol, 15*. This synthesis was carried out from nitrophenylamino-D-mannitol **1** following two steps. (1) Compound **1** (0.85 g, 3 mmol) was dissolved in a solution of methanol; Pd/C 10% (0.15 g) was added, and the reduction was achieved by hydrogenation (at atmospheric pressure, room temperature, 1 h). Filtration and evaporation yielded the amino derivative as a colorless oil (0.75 g, 2.97 mmol, yield 99%). ^1H NMR (CD_3OD , δ): 6.86 (t, 1H, $J_{10,11} = J_{11,12} = 8.7$ Hz, H-11), 6.13–6.07 (m, 3H, H-8, H-10, H-12), 3.94 (m, 3H, H-2, H-4, H-5), 3.81 (m, 1H, H-3), 3.74–3.58 (ABM syst, 2H, $J_{5,6} = 5.8$ Hz, $J_{6a,6b} = 11.8$ Hz, H-6a, H-6b), 3.34–3.19 (ABM syst, 2H, H-1a, H-1b); ^{13}C NMR (CD_3OD , δ): 151.06 (C-7), 149.26 (C-9), 130.72 (C-11), 106.91, 105.70 (C-10, C-12), 101.91 (C-8), 85.19 (C-5), 83.24 (C-2), 80.65 (C-3), 79.05 (C-4), 63.39 (C-6), 44.68 (C-1); MS (DCI, NH_3) m/z : 255 [$\text{M} + \text{H}$] $^+$.

(2) Thiophosgene (0.1 mL, 1.1 mmol) in chloroform (4 mL) was dropped into a solution of the amino derivative (0.23 g, 0.92 mmol) dissolved in ethyl acetate at 0 °C. After stirring for 3 h at room temperature, the solvents were evaporated, and the resulting syrup was purified by flash chromatography ($\text{CH}_2\text{Cl}_2/\text{MeOH}$ 95:5). Compound **15** was a pale-yellow oil (0.046 g, 0.15 mmol, yield 17%). IR: 2092.9 cm^{-1} ($\text{N}=\text{C}=\text{S}$); ^1H NMR (CD_3OD , δ): 7.09 (t, 1H, $J_{10,11} = J_{11,12} = 7.97$ Hz, H-11), 6.61 (dd, 1H, $J_{10,11} = 7.97$ Hz, $J_{10,12} = 1.6$ Hz, H-10), 6.51 (m, 2H, H-8, H-12), 3.97 (m, 3H, H-2, H-4, H-5), 3.86 (m, 1H, H-3), 3.74–3.58 (ABM syst, 2H, H-6a, H-6b), 3.33–3.24 (ABM syst, 2H, H-1a, H-1b); ^{13}C NMR (CD_3OD , δ): 189.84 (C-13), 151.37 (C-7), 133.03 (C-9), 131.24 (C-11), 114.96 (C-10), 113.59 (C-12), 110.02 (C-8), 85.13 (C-5), 83.09 (C-2), 80.81 (C-3), 78.89 (C-4), 63.35 (C-6), 46.78 (C-1); MS (DCI, NH_3) m/z : 297 [$\text{M} + \text{H}$] $^+$.

Assay of Enzyme Activities. The phosphotransferase activity of PFK was followed spectrophotometrically as the oxidation of NADH by linking the formation of one of the reaction products, either F1,6P or ADP–Mg, to this oxidation in the presence of an excess of auxiliary enzymes: for F1,6P with aldolase, TIM, and GPDH (method A); for ADP–Mg with PyK, and LDH (method B). In method A, the reaction mixture (1 mL) contained 0.1 M triethanolamine hydrochloride buffer (pH 7.6), 1 mM EDTA, 0.6 mM NADH, 0.5 mM ATP, 2.5 mM MgCl_2 , 1 mM NaHCO_3 , 2 mM F6P, 1.6 mM AMP, 100 μg of aldolase (0.9 units), 10 μg of TIM (5 units), and 10 μg of GPDH (1.7 units). In method B, the reaction mixture (1 mL) contained 0.1 M triethanolamine hydrochloride buffer (pH 7.6), 1 mM EDTA, 0.42 mM NADH, 2.2 mM PEP, 0.5 mM ATP, 2.5 mM MgCl_2 , 1 mM NaHCO_3 , 1.6 mM AMP, and 2.5 μL of 1/1 PyK/LDH (1.1 units). All reactions were carried out at 25 °C. The decrease of NADH was measured at 340 nm with a PerkinElmer spectrophotometer equipped with a kinetics accessory unit. Steady-state kinetic parameters were evalu-

Table 1: Michaelis Constants and Kinetic Parameters of the Overexpressed Tb-PFK

Michaelis constants		kinetic parameters	
$K_m^{\text{ATP-Mg}}$	144 μM	V_m	45.5 $\mu\text{mol min}^{-1}$
$K_s^{\text{ATP-Mg}}$	37 μM	k_{cat}	196 s^{-1}
K_m^{F6P}	1150 μM	K_1	$1.36 \times 10^6 \text{ s}^{-1} \text{ M}^{-1}$
K_s^{F6P}	850 μM	K_{-1}	50.3 s^{-1}
		K_2/k_{-2}	$1.70 \times 10^5 \text{ s}^{-1} \text{ M}^{-1}$

ated by direct fit of initial velocity data versus substrate concentration to the Michaelis–Menten equation using a weighted nonlinear regression method in the program for Windows. Initial reaction rates were calculated from the slopes of the curves recorded during the first 3 min of the reaction and from the NADH concentrations using $\epsilon_{340} = 6.22 \text{ mM}^{-1} \text{ cm}^{-1}$. Individual initial rates were kept only when they corresponded to values obtained with correlation coefficient equal to or better than 0.998

Inactivation Studies. The inhibitory activities of compounds on PFK were measured after preincubation of the enzyme with the compound for 5 min followed by the addition of the reaction mixture to trigger off the reaction. A possible effect of the inhibitors on the absorbance of NADH was checked and no effects on the enzyme activity were observed at solvent (dimethyl sulfoxide) concentrations below 10%. The concentration of inhibitor required for 50% inhibition (IC_{50}) was calculated from five different inhibitor concentrations and saturating conditions of the substrates. Initial velocity was determined from the continuous time course by extrapolation of the linear position of the curve to zero time, so the rates reflected conversion of less than 10% of the limiting substrate. IC_{50} values were then estimated from a semilog plot of inhibitor concentration versus percent inhibition of enzyme activity.

Inhibition Studies. Inhibition experiments were performed like activity assays but in the presence of 1.5 mM AMP, with variable concentrations of inhibitor and one of the substrates, while the second substrate concentration was saturating. The inhibition with respect to F6P was studied at four different F6P concentrations (330, 165, 100, and 75 μM) at a saturating concentration of ATP (1 mM). Inhibition with respect to ATP was studied at four different ATP concentrations (330, 165, 100, and 75 μM) at a saturating concentration of F6P (2 mM). AMP inhibition was studied at five different ATP concentrations (150, 200, 330, 400, and 500 μM). Kinetic constants were determined by nonlinear regression assuming Michaelis–Menten kinetics. Inhibition constants (K_i and K_{ii}) are reported as means \pm the standard error of representative experiments performed in triplicate. Data are represented as double reciprocal plot $1/v$ versus $1/S$ (Lineweaver–Burk plot) for illustrative purposes (21). Although it was shown that the histidine tag does not interact with substrates (Table 1), a possible interaction with inhibitors cannot be ruled out. In this event, experimental affinities would be underestimated.

Fluorescence Measurements. All fluorescence spectra were made at 20 °C in 4-mL clear-sided cuvettes using a PerkinElmer LS-50B spectrometer. For quenching experiments, tryptophan fluorescence was excited at 295 nm. Excitation and emission spectra were recorded with slits set at 5 nm. For dissociation constants, various intensities were

used at 330 nm. All fluorescence studies were performed in 0.1 M triethanolamine/HCl buffer (pH 7.5) with a PFK concentration of 6.5 μM and variable quencher concentrations between 0 and 250 mM.

Quenching data (Q and K_d) were analyzed by a least-squares fit to the Stern–Volmer equation, and the accessibility (f_a) of tryptophan residues to quenchers was calculated by use of a modified Stern–Volmer equation (22). Estimates of K_d and f_a were obtained by using linear regression analysis with Microcal Origin 4.00 (Microcal Software Inc., Northampton, MA).

Circular Dichroism Spectra. CD spectra were collected on a Jobin-Yvon CD6 spectropolarimeter with 1 mm path at 25 °C, under a flux of nitrogen. The data were collected from 195 to 260 nm. They were the average of at least two blank-corrected samples and were corrected to correspond to an absorbance of 1.0 in a 1-cm spectrophotometer. Before assay, the enzyme was dialyzed and diluted to a concentration of 1 mg/mL.

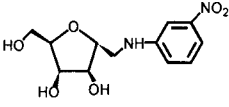
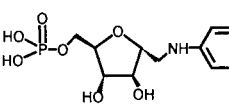
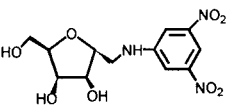
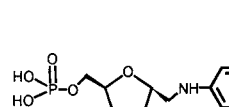
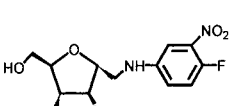
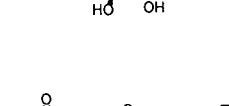
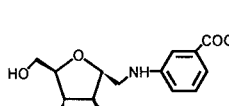
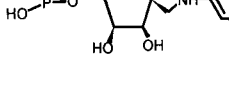
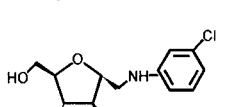
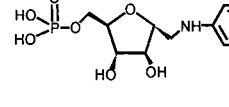
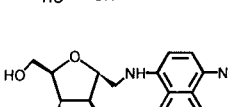
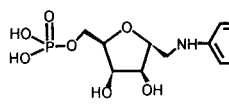
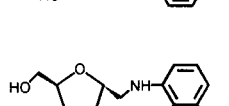
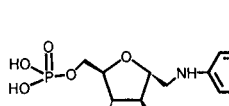
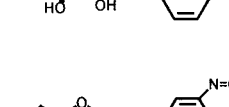
RESULTS

Kinetic Parameters and Michaelis Constants of the Overexpressed *T. brucei* PFK. Effect of substrate concentration on the initial rates of the reaction were used to determine the kinetic constants for the reaction catalyzed by the overexpressed *T. brucei* PFK (Table 1). They are very similar to those previously reported (9–11). As for the natural parasite enzyme, the velocity of *T. brucei* PFK displays a sigmoidal dependence on F6P at low substrate concentration (<0.3 mM). In the presence of AMP (1.5 mM), the maximum velocity of the reaction increases and the enzyme exhibits a Michaelis–Menten type behavior. To be able to interpret the effect of inhibitory compounds unambiguously, it was first necessary to get a better understanding of the role of AMP. This was obtained by examining the action of the effector concentration on the maximum velocity. (i) AMP, in the concentration range 0.5–1.5 mM, has no inhibitory effect with respect to both substrates. Inhibition by AMP requires substrate concentrations higher than 5 or 10 times the corresponding K_m values, 2 mM for F6P, and 0.5 mM for ATP. (ii) For F6P concentrations higher than 2 mM, inhibition with respect to this substrate is clearly partial. (iii) When the concentration of AMP is varied from 0.25 to 0.75 mM, it displays a noncompetitive inhibition pattern with respect to high ATP concentrations. Under these conditions, the K_i of AMP for the free enzyme and the K_i' of AMP for the enzyme–ATP complex had the same value (1.5 mM) corresponding to a low affinity. For ATP, the affinities were identical for the free enzyme and for the enzyme–AMP complex and were close to the K_m^{ATP} for the enzyme ($K_s = K_s' = 125 \mu\text{M} = K_{m \text{ app}}$).

This inhibitor behavior, together with that of activator observed at low substrate concentrations, is qualitatively consistent with the V_m variation theory according to Cleland (23): (i) influence of AMP just depends on ATP concentration, and (ii) whatever this concentration may be, the effector was found to modify the maximum velocity of the reaction without affecting the substrate affinity.

Design of Inhibitors and Inactivation Study. Inhibitors were designed from the reference structure 2,5-anhydromannitol, an analogue of fructose blocked in a closed conforma-

Table 2: Effect of Compounds on *T. Brucei*-PFK: Structure and IC₅₀ Values for Saturating and NonSaturating Concentrations of ATP-Mg and F6P^a

composé	IC ₅₀ (mM)			composé	IC ₅₀ (mM)		
	ATP et F6P saturants	/ATP	/F6P		ATP et F6P saturants	/ATP	/F6P
 1	1.1	0.47	0.44	 8	0.45	0.39	--
 2	1	0.47	0.92	 9	0.66	0.40	--
 3	1.1	0.45	--	 10	0.72	0.65	--
 4	1.2	0.65	--	 11	0.8	0.60	--
 5	1.5	0.75	--	 12	0.53	0.3	--
 6	1	0.51	1	 13	1.5	0.33	--
 7	0.9	0.36	0.4	 14	1.5	0.43	--
 15	0.5	0.16	0.5				

^a Saturating concentrations: 1 mM for ATP-Mg and 2 mM for F6P. The inhibition with respect to one substrate was studied at concentration of $K_m = 50 \mu\text{M}$ for ATP-Mg and $150 \mu\text{M}$ for F6P. (--) No effect at 5 mM. Each determination was done in triplicate with SD $\pm 4\%$.

tion. This structure was varied by linking a diversely substituted aromatic ring through a nitrogen atom attached at position 1 and phosphorylating at position 6. Substitution at the meta position was chosen to explore a larger area of the enzyme's active site by ring rotation. It was observed that the aromatic ring was required for inhibition; indeed 2,5-anhydromannitol bearing either $-\text{COOCH}_3$, $-\text{CH}=\text{CHCOOCH}_3$ (introduced as a possible Michael acceptor), $-\text{NH}_2$, or $-\text{COOH}$ at position 1 gave no inhibition. Noteworthy is the fact that F6P analogues, 2,5-anhydromannitol bearing groups $(\text{HO})_2\text{P}(\text{O})\text{CH}_2\text{NH}$ or $(\text{HO})_2\text{P}(\text{O})\text{CH}(\text{OH})$ at position 1, gave no inhibition and did not behave as pseudosubstrates (as seen from the kinetic study with method B). These phosphorylated compounds could indeed be considered as pseudosubstrates of PFK because positions 1 and 6 are equivalent, owing to the transformation of either

structure into the other by a C2 rotation. For aromatic derivatives, the corresponding structures and IC₅₀ values with respect to both substrates are given in Table 2. For compounds bearing one or two polar groups, inhibition was observed only if groups on the aromatic ring were negatively charged or corresponded to a dipole with an external negative part. Compounds equivalent to **1** or **8**, with an amino group in place of the nitro group, gave no inhibition.

Inhibition Kinetics. For inhibitors having an IC₅₀ value lower than 1.2 mM, the nature of the inhibition with respect to both substrates is reported in Table 3.

(i) **Reversible Inhibition with Respect to F6P.** For compound **6**, the Lineweaver-Burk reciprocal plots intersect on the $1/v$ axis at any concentration of the inhibitor, showing that this compound competes with the F6P substrate. For compounds **1** and **7**, the plots intersect at the left of the $1/v$

Table 3: Inhibition Pattern with *T. Brucei* PFK as Analyzed by Lineweaver–Burk Plots^a

no.	with respect to F6P			with respect to ATP			with respect to ATP		
	type of inhibition	K (μ M)	type of inhibition	K (μ M)	K_d (μ M)	no.	type of inhibition	K (μ M)	
1	FM	$K_i = 750 \pm 20$, $K_s = 305 \pm 10$, $K_i' = 275 \pm 12$, $K_s' = 110 \pm 8$	C	$K_i = 390 \pm 9$	40 ± 2	8	C	$K_i = 250 \pm 9$	
2	NC	$K_i = K_i' = 390 \pm 12$, $K_s = K_s' = 250 \pm 8$	C	$K_i = 320 \pm 8$	68 ± 6	9	C	$K_i = 150 \pm 7$	
3						10	C	$K_i = 122 \pm 4$	
4			C	$K_i = 165 \pm 5$	71 ± 7	11	C	$K_i = 310 \pm 16$	
6	C	$K_i = 500 \pm 25$	NC	$K_i = K_i' = 450 \pm 13$	65 ± 5	12	C	$K_i = 140 \pm 12$	
7	FM	$K_i = 410 \pm 17$, $K_s = 220 \pm 10$, $K_i' = 250 \pm 11$, $K_s' = 100 \pm 5$	PM		64 ± 5	13	FM	$K_i = 400 \pm 25$, $K_i' = 600 \pm 52$	
			PM		67 ± 5				

^a (C) Competitive, (NC) noncompetitive, (FM) fully mixed-type, (PM) partially mixed-type. K_d from spectrofluorometry measurements with $K_d^{\text{ATP}} = 39 \mu\text{M}$.

axis, below the $1/[\text{F6P}]$ axis; intercepts and slopes versus concentration are linear. These two compounds act as fully mixed-type (FM) inhibitors, with $K_i'/K_i < 1$ and $K_s/K_s' < 1$ (dissociation constants for F6P of the ES and ESI complexes). Compound **2** is a noncompetitive inhibitor with $K_i = K_i'$ and $K_s = K_s'$.

Reversible Inhibition with Respect to ATP–Mg. The following four kinds of kinetic behavior were observed. (i) For the nitro compounds **1–3**, the Lineweaver–Burk reciprocal plots intersect on the $1/v$ axis and the replots of slopes versus inhibitor concentrations allow for the determination of K_i values of competitive inhibition. (ii) For naphthylamine derivatives **6** and **7**, the double reciprocal plots are linear but plots of apparent K_m/V and $1/v$ are curved downward, the limits which should allow for the determination of K_i values which are difficult to reach. This partially mixed inhibition accounts for a system where more than one inhibitor molecule can bind to the same molecule of enzyme, leading to a productive ternary complex (24). (iii) With compound **4**, the reciprocal plots intersect on the abscissa; this noncompetitive inhibition shows linear replots of slopes and intercepts against inhibitor concentrations that give $K_i = K_i'$. (iv) Compound **13** exhibits a particular noncompetitive inhibition pattern with a reciprocal plot that intersects below the $1/[\text{ATP}]$ axis giving $K_i' > K_i$.

Enzymatic Reaction Mechanism. Comparison of different kinetic and affinity constants (K_i and K_s) of inhibitors acting at steady-state concentrations of both substrates can provide information as to how, in the formation of a multiple complex, the concentration of one substrate affects the affinity for the other (25, 26). This is illustrated for *T. brucei* PFK by the following observations. (i) Compounds **1** and **2** are competitive with respect to ATP with identical K_i values. Their dissociation constants for the free form of the enzyme, $K_d = 40 \mu\text{M}$ for **1** and $K_d = 68 \mu\text{M}$ for **2**, are very close to the K_d value of ATP for the protein ($30 \mu\text{M}$). (ii) With respect to F6P, compounds **1** and **2** give two patterns: (1) a fully mixed-type for compound **1**, with an important uncompetitive component ($K_i \approx 3K_i'$); the affinity constant values of F6P for the enzyme–ATP complex ($K_s = 305 \mu\text{M}$) and for the enzyme–inhibitor–ATP complex ($K_s' = 110 \mu\text{M}$) are lower than those of F6P for the free enzyme ($K_s = 850 \mu\text{M}$); and (2) noncompetitive inhibition for compound **2**, with $K_i = K_i'$ and $K_s = K_s'$, giving a better affinity of F6P for the enzyme–ATP and enzyme–inhibitor–ATP complexes than for the free enzyme. (iii) Compounds **7** and **6**, which behave

as partially mixed-type inhibitors with respect to ATP, revealed that multicomplexes exist under nonsaturating ATP concentrations. Together, these data show that the inhibitors bind to the free enzyme as ATP analogues with the same affinity as this substrate and that binding of the inhibitors increases the affinity of F6P for the protein.

Kinetic Data. The entire set of kinetic data indicates that this series of inhibitors act as ATP analogues for PFK. This inhibition is specific for this enzyme because these derivatives do not inhibit ATP binding to other kinases, such as hexokinase or pyruvate kinase (results obtained with the *T. brucei* enzymes; not shown). The noncompetitive patterns observed for compounds **1**, **2**, **6**, and **7** at variable F6P concentrations provide a better insight into the behavior of these inhibitors at extreme ATP concentrations. For compound **2**, the affinity values are weakly modified by the ATP concentrations: $K_i' = 390 \mu\text{M}$ with ATP at saturating concentrations and $K_i = 320 \mu\text{M}$ with ATP at concentrations near its K_m value. In contrast, the affinity of compound **7** for the protein is reduced in the presence of high ATP concentrations, $K_i' \approx 2K_i$. Even at variable ATP concentrations, the uncompetitive effect is observed for compounds **4** and **13**, with $K_i = K_i'$ and $K_i = 0.66K_i'$, respectively, consistent with the formation of an unproductive quaternary complex E–F6P–ATP–I. These data show that ATP does not prevent the association of these compounds with the enzyme in its active site; but very likely, they are not bound in exactly the same environment as ATP.

(ii) **Irreversible Inhibition.** Two inhibitors bearing an electrophilic center at the meta position of the aromatic ring, either a bromoacetamidyl or an isocyanate group, might covalently link to the protein by interacting with a basic residue at the active site. Whereas no effect was observed with the acetyl bromo derivative, preincubation of compound **15** with the enzyme led to time-dependent inactivation by a pseudo-first-order inactivation process (Figure 1A). This irreversible effect was confirmed by the fact that no enzymatic activity was recovered after dilution of the enzyme–inhibitor mixture obtained after the incubation time and also by protection in the presence of substrates. The dissociation constant of the reversible enzyme–inhibitor complex was $K_i = 133 \mu\text{M} \pm 7$, and the inactivation rate constant for the formation of the covalent bond between enzyme and inhibitor was $k_i = 0.026 \text{ min}^{-1} \pm 0.002$.

Mutagenesis and Identification of the Residue Involved in the Covalent Binding of Compound 15. Residues Lys226

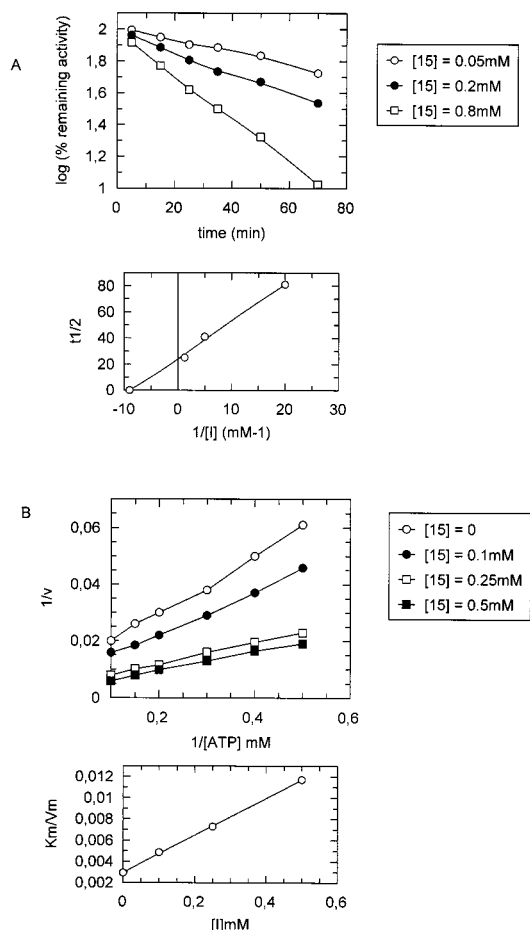


FIGURE 1: (A) Inactivation of *T. brucei* PFK by compound **15**. Logarithm of the percentage of the remaining PFK activity at varied inhibitor concentrations versus time. (Lower panel) Replot of the half-inactivation time against the reciprocal inhibitor concentrations and determination of the inactivation constant k_{second} and K_i . (B) Inactivation of Lys227Gly mutant of *T. brucei* PFK by compound **15** at different inhibitor concentrations. (Lower panel) Secondary plot and determination of the inhibition constant K_i .

and Tyr139 were selected because they take into account the following features. (i) Tyr139 is the only residue identified in the adenine binding pocket able, by virtue of its OH group, to react with the electrophilic isocyanate group. Indeed, Arg77 giving a hydrophobic interaction with adenine in *E. coli* PFK is deleted in the *T. brucei* enzyme (gap 74–78, see Figure 3 inside ref 15). (ii) Lys226 is highly conserved in all PPKs, whereas a glycine is found at the corresponding position in the ATP–PFKs. The specific activities of the purified mutated enzymes Lys226Gly (100 U mg⁻¹) and Tyr139Phe (125 U mg⁻¹) were very similar to that of the wild-type enzyme (110 U mg⁻¹), and their Michaelis constants were not altered. The minor loss of affinity for ATP observed in the Lys226Gly mutant (220 μ M against 90 μ M for the wild-type enzyme) indicates the importance of Lys226 for the binding of ATP. Assays of these two mutated enzymes with inhibitor **15** led to the following results. Mutant Tyr139Phe showed exactly the same pattern of inhibition as the wild-type PFK: a similar time dependence with a 2-fold lower affinity ($K_i = 236 \mu\text{M}$) and a rate constant in the same range $k_i = 0.018 \text{ min}^{-1} \pm 0.002$. In contrast, the inhibition kinetics with mutant Lys226Gly show a fully noncompetitive reversible inhibition

with $K_i = K_i' = 185 \mu\text{M}$ (Figure 1B). This indicates that Lys226 is responsible for the covalent link between the inhibitor and the protein.

Fluorescence Spectroscopy. Quenching of the Intrinsic Fluorescence of PFK, at Fixed Wavelength (330 nm). The shape and the frequency of the PFK fluorescence band is a sensitive probe for the conformational state of the protein (28, 29). When following the fluorescence of the ligand-free enzyme (Table 4), ATP acts as a quencher that allows for the identification of four accessible tryptophans to this substrate, while only two residues are evidenced by addition of F6P. With the charged iodide quencher, the plot of the fluorescence intensity versus quencher concentration is linear and yields an accessible fraction value ($f_a = 48\%$), corresponding to six exposed tryptophan residues. With acrylamide, a similar plot exhibits a downward curvature, indicating the presence of two populations of tryptophans. At saturating concentrations of the quencher, in the absence of substrates, the accessible fraction is about 80%, giving 10 accessible tryptophans. For both PFK–ATP and PFK–F6P binary complexes (Table 4), six tryptophan residues are characterized by iodide quenching, whereas seven are accessible to acrylamide; this indicates that six or seven tryptophan residues of the enzyme are fully exposed to the solvent and that their accessibility is not modified by the binding of either substrate to the enzyme. Owing to the four tryptophans quenched by ATP, the total number of tryptophans affected by the binding of ATP is 10 with iodide and 11 for quenching by acrylamide. These results suggest that one or two tryptophan residues are buried, owing to the assembly of the tetrameric enzyme, while one tryptophan per subunit seems to be specifically influenced by the binding of ATP. The buried tryptophan is likely near the binding site of the ATP ($f_a = 37\%$ with ATP) and essentially contributes to quenching the fluorescence when the protein conformation is modified by the binding of ATP.

Fluorescence Spectra (300–400 nm). When the enzyme was loaded with 10 mM of ATP, the binding of ATP to the PFK increased the overall fluorescence emission up to 24% (Figure 2A, trace b), suggesting a structural organization of the protein by the binding of the substrate (29). On the contrary, the fluorescence emission of PFK is quenched by iodide and to a larger extent by acrylamide, with or without ATP. To identify the wavelength associated with the tryptophan the environment that is modified by substrate binding, the difference spectra between the PFK–ATP complex and PFK alone, with or without quencher, were plotted (Figure 2B). From the difference spectrum between PFK–ATP complex and PFK alone (Figure 2B, trace a), two components at 328 and 331 nm were identified as positive contributions. These two components (slightly shifted to 325 and 328 nm) were still detected when acrylamide was added to the PFK–ATP complex (Figure 2B, trace b). These results suggest that the fluorescence should be ascribed to tryptophan residues moderately exposed to the solvent, located near the binding site of ATP. The sequence alignments of *T. brucei* and *E. coli* PFK and the 3D structure of *E. coli* PFK (30) suggest that Trp142 is a potential candidate.

Dissociation Constants and Percentage of Quenching. For inhibitors, the K_d values were between 61 and 78 μM (Table 3), 2-fold higher than the K_d value of ATP ($K_d = 30 \mu\text{M}$), except for compound **1** which had the same K_d as the

Table 4: Acrylamide and Iodide Quenching, (f_a) Accessible Fraction, and (n_{TTP}) the Number of Tryptophan Residues Accessible to the Quencher

	PFK				PFK-ATP		PFK-F6P	
	ATP	F6P	iodide	acrylamide	iodide	acrylamide	iodide	acrylamide
f_a (%)	37 ± 4	18 ± 2	48 ± 4	78 ± 10	49 ± 5	60 ± 5	52 ± 3	55 ± 4
n_{TTP}	4	2	6	10	6	7	6	7

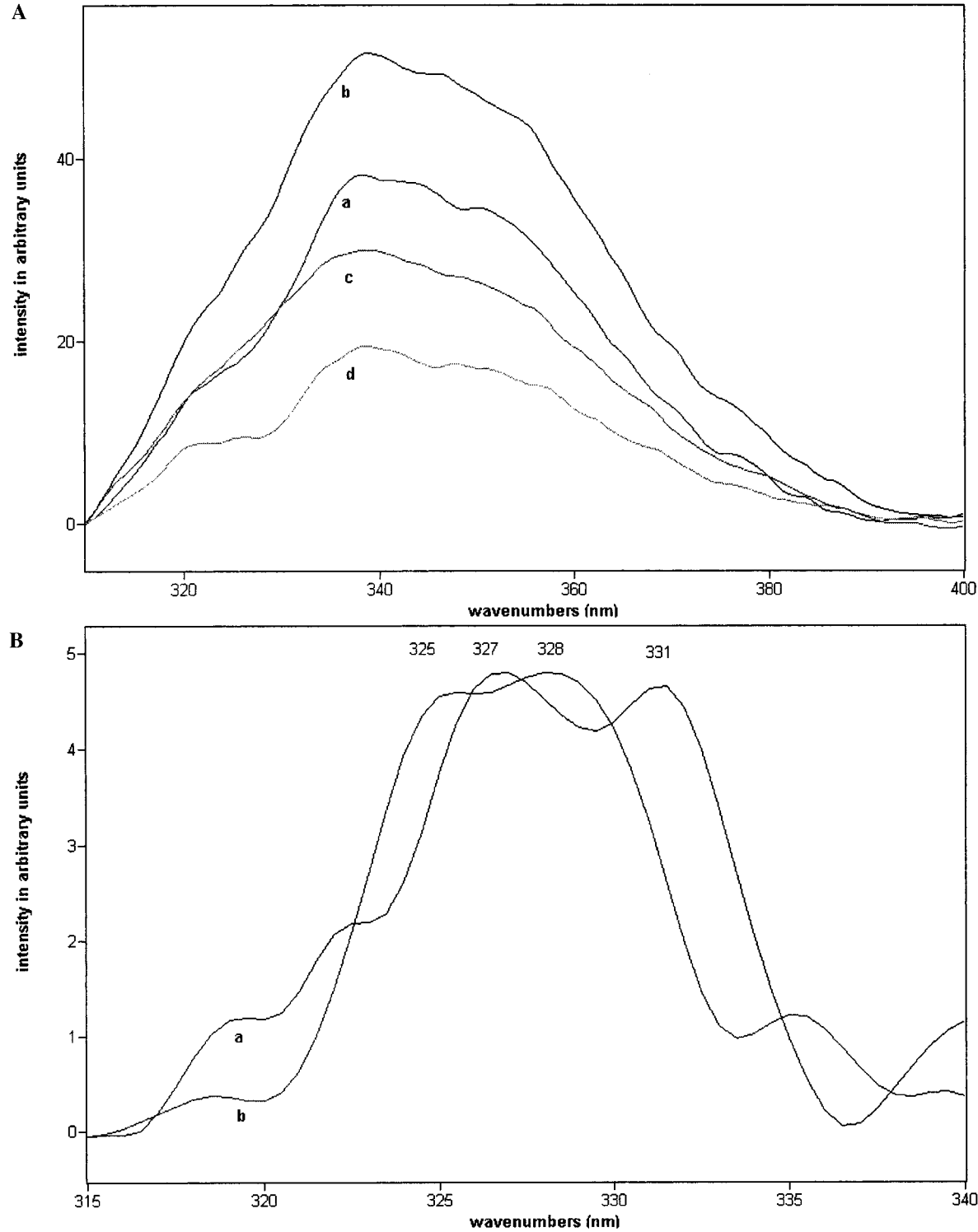


FIGURE 2: (A) Fluorescence spectra of *T. brucei* PFK: (a) PFK alone, (b) PFK-ATP (50 mM), (c) PFK-IK (150 mM), and (d) PFK-acrylamide (150 mM). (B) Difference spectra of *T. brucei* PFK: (a) PFK/ATP-PFK, and (b) PFK/ATP/acrylamide-PFK/ATP.

ATPMg-PFK complex. For ATP analogues, adenosine was more tightly bound than AMP or ATP itself (Table 5).

Quenching of the intrinsic fluorescence of *T. brucei* PFK was 21–30% with ATP and analogous molecules (ATP–

Table 5: Dissociation Constants (K_d) and Percentage of Quenching of Fluorescence (Q_{\max}) of *T. Brucei* PFK for ATP and Its Analogues

	K_d (μ M)	Q_{\max} (%)		K_d (μ M)	Q_{\max} (%)
ATP-Mg	30 \pm 2	30 \pm 1	adenosine	16 \pm 0.5	21 \pm 0.5
ATP	39 \pm 3	29 \pm 0.5	AMPPCP-Mg	33 \pm 2	44 \pm 2
AMP	29 \pm 1	21 \pm 0.5			

Mg complex, AMP, adenosine) while all inhibitors strongly decreased the fluorescence intensity of PFK ($Q\%$ 56–85). The nonhydrolyzable ATP analogue, AMP-PCP, gave an intermediate result with 44% of quenching, consistent with its weak inhibitory effect on kinases and particularly PFKs (31).

Circular Dichroism Spectroscopy. The addition of F6P had no significant effect on the reference spectrum; when ATP was added, the intensity of the minimum at 208 nm decreased and the minimum at 222 nm shifted to 218 nm, with an increase in intensity. ATP changed the conformation of the protein by decreasing the percentage of the α -helix structure (Figure 3A). Compound **10**, fully competitive with respect to ATP with a $K_i \cong K_m$, gives rise to a spectrum which is almost superimposable on that of ATP (Figure 3B). The spectrum of the compound **13**–PFK complex shows a 50% decrease of the α -helix structure (195 nm) with formation of a disordered structure (198 nm) (Figure 3C). These observations can be accounted for (i) by a possible interaction of the aromatic ring of the noncompetitive inhibitor **13** with hydrophobic residues, generally buried in helix structure, a partially denaturing of the protein; and (ii) by the importance of nitro groups of the competitive inhibitor **10**, to promote an essential contact with residues involved in ATP binding.

DISCUSSION

We first confirmed that the recombinant *T. brucei* PFK had the same values for its kinetic parameters (Table 1) as the natural enzyme purified from parasites with a sigmoidal behavior at low F6P concentrations (9–11). The 20-residue tag attached to the N-terminus does not introduce any significant change in the kinetics. The mechanistic behavior of *T. brucei* PFK could be completed and compared to those of other ATP-dependent PFKs. Indeed, different previously established pathways were possible: for the rabbit muscle enzyme, for instance, a rapid-equilibrium random-bireactant system (32, 33) has been identified, whereas, for *E. coli*, the concerted mechanism is random and nonequilibrating (34–36). In the case of *T. brucei* PFK, the use of inhibitors such as **1**, **2**, **6**, and **7**, the inhibitory kinetic studies with AMP, and the fluorescence experiments enabled us to reach a conclusion. Under steady-state conditions with respect to both substrates, (i) it was found that inhibitors that compete with ATP bind at the ATP binding site with a dissociation constant close to the K_d^{ATP} value; this affinity of ATP for the enzyme, measured by fluorescence spectroscopy, is decreased in the presence of these inhibitors; (ii) in contrast, the affinity of F6P for the enzyme–inhibitor complexes is increased. Clearly, the inhibitors play the same role as ATP (or AMP) in increasing the affinity of the second substrate F6P for the enzyme. This implies that the mechanism of *T. brucei* PFK is ordered, with ATP binding first to the enzyme. Moreover, the detailed kinetic analysis of this enzyme with respect to the effector AMP and also the circular dichroism

analysis show that AMP does not modify the affinity of ATP for the enzyme but plays a role similar to that of ATP in inducing an essential conformational change. This conformational change corresponds to a structural organization of the enzyme toward its active form by the binding of its substrate, as shown by the increase of the overall fluorescence for the PFK–ATP complex.

A strategy for the synthesis of a series of inhibitors was developed with the aim of simplifying the route as much as possible because the compounds described in this paper are considered intermediates in the long-term aim of developing highly selective high-affinity inhibitors. The whole study of *T. brucei* PFK inhibition by these substrate analogues led to the following observations. (i) The molecules very close in structure to F6P such as 2,5-anhydro-D-mannitol phosphorylated at position 6 are not inhibitors, whereas 2,5-anhydro-D-mannitol-6P is substrate for both rat liver and rabbit muscle ATP–PFKs (37). Also, the replacement of the alcohol function by an acid, an amide, an ester, or an activated electrophile did not make an inhibitor. (ii) Owing to the C2 symmetry axis of the 2,5-anhydro-D-mannitol, this set of molecules keeps a sugar moiety which could be phosphorylated by the kinase, but the kinetic study did not reveal ADP formation, ruling out the possibility that they are pseudosubstrates. (iii) On the contrary, for all other compounds (phosphorylated or not) where a hydrophobic contribution was introduced via an aromatic ring, an inhibitory effect was observed. IC_{50} values for the two series of inhibitors reveal that the nonphosphorylated ones inhibit with respect to both substrates F6P and ATP, whereas phosphorylated analogues only inhibit with respect to ATP.

For the nonphosphorylated compounds, the detailed kinetic analysis, showing a general effect of noncompetitive inhibition with respect to both substrates, indicates that these compounds preferentially bind to the ATP site: (i) an essential uncompetitive component where the highest affinities are for the F6P–enzyme complex; (ii) the K_i values are lower with respect to ATP; and (iii) their K_d values are very close to that of the ATP–Mg complex itself (39 μ M).

For the phosphorylated derivatives, the kinetics with respect to ATP are, in all cases, fully competitive. The affinity for this site is improved compared to that of the corresponding nonphosphorylated compounds, and the value of the ratio K_i/K_m^{ATP} is about 1. This selectivity of binding at the ATP site was also supported by CD spectroscopic studies: (i) inhibitor **10**, which only binds at the ATP site, gives a spectrum that can be superimposed on that obtained with ATP, indicating a conformational change similarly induced by both compounds; and (ii) inhibitor **13**, which gives a mixed-type inhibition, induces a partial denaturation (unfolding) of the protein as shown by the increase of the percentage of random structures.

The highest affinities were found for compounds bearing either a negative charge or an electron-withdrawing group on the ring. Corresponding to this ionic contribution, it was considered that if the residue, likely a lysil, responsible for interaction with the inhibitor has a pK value close to the physiological pH value, it could become, in the unprotonated form, a reactive nucleophile. This turned out to be the case, because an irreversible inhibitor was developed. It is noteworthy that the ATP-binding site is a rather hydrophobic environment, which may account for a high reactivity of the

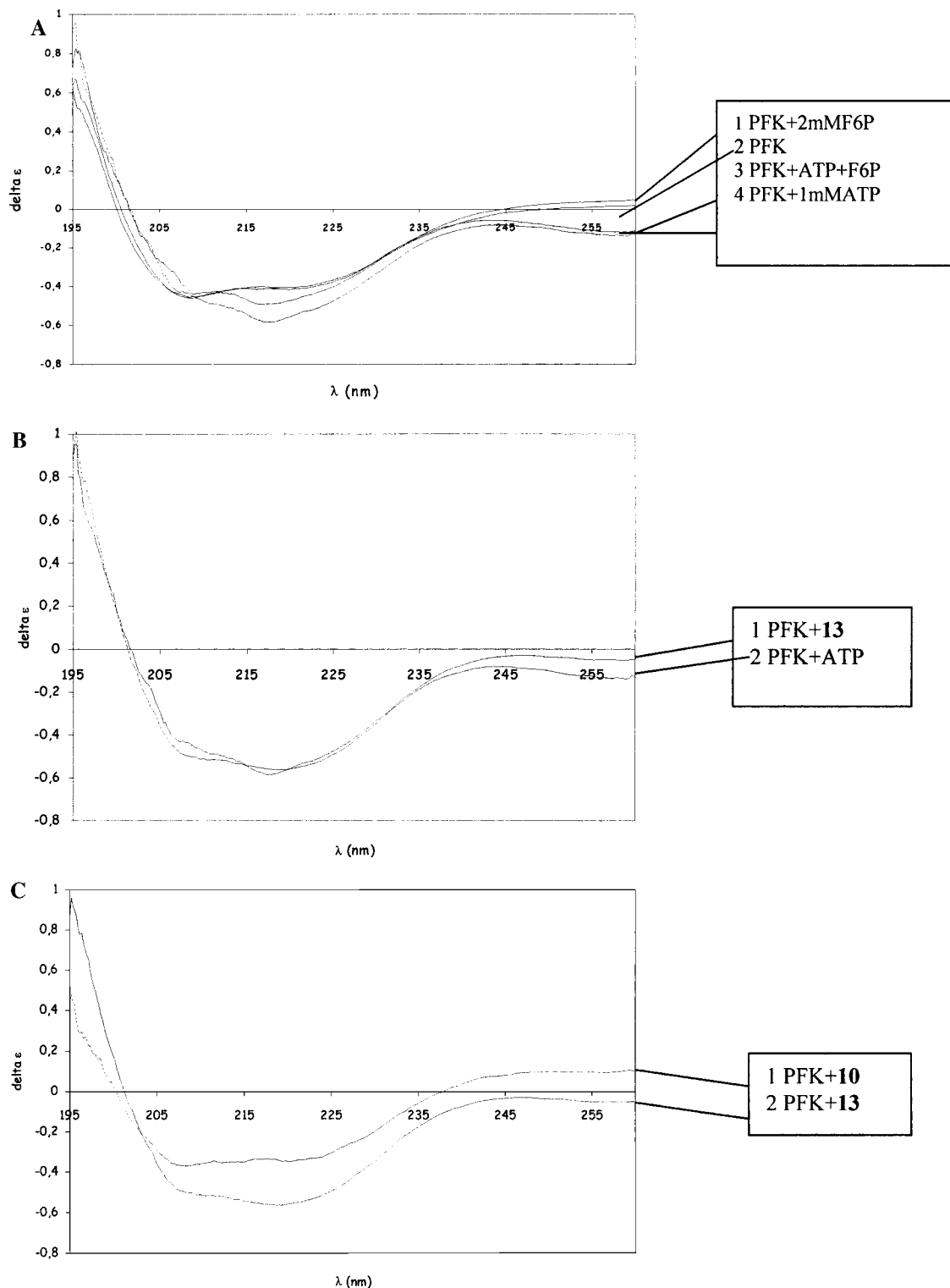


FIGURE 3: Circular dichroism spectra of binary complexes between *T. brucei* PFK and its substrates or inhibitors **10** and **13**.

lysyl residue due to the absence of solvation and a lowering of its pK . Whereas the adenosine part of ATP makes five hydrophobic contacts with the active site of *E. coli* PFK and two hydrogen bonds with Arg82 and Arg111, it can be inferred from multiple sequence alignment that the interactions in the *T. brucei* enzyme, where the two arginine residues have been substituted for proline and valine, respectively, are more likely only hydrophobic (15). This proposal is also confirmed by fluorescence experiments where K_d and $Q\%$ values for inhibitors indicate their binding

at the ATP site with similar affinity. Moreover, K_d values of ATP analogues show (Table 5) that the more hydrophobic they are, the higher their affinity. Finally, as evidenced by fluorescence experiments, the presence of Trp142 contributes to the hydrophobic character of the ATP binding site.

On the basis of this information, two analogues of compounds **13** with an electrophilic center (bromomethyl-amido and isocyanate groups) at the meta position were synthesized and assayed. Irreversible inhibition was only observed for the isothiocyanate group of compound **15** with

the best K_i value (133 μ M) in the series. This indicates that a nucleophilic residue must be located in the protein to react on an electrophilic center in a β position with respect to the meta carbon atom on the aromatic ring, but not if the electrophilic center is in a γ position. Lys226 was identified as the active nucleophile because the mutation Lys226Gly was found to prevent the irreversible inhibition by compound **15**. Surprisingly, the affinity of **15** for the Lys226Gly mutant keeps a significant value, close for instance to the K_i value of analogue **3** for the wild-type enzyme. This suggests the presence of another basic residue near Lys226. In accordance with this, the presence of a highly conserved aspartic acid (Asp229 in *T. brucei*, Asp127 in *E. coli*), close to this lysine, is noticeable in all ATP-dependent PFKs. This aspartic acid, which plays a role as general base around the γ -phosphate as demonstrated by Hellinga and Evans (38), could be involved in binding the inhibitor in the absence of Lys226. The fact that this lysyl group reacts on inhibitor **15** is of great significance; indeed, in the human enzyme, this residue is replaced by a nonreactive glycine; therefore, compound **15** is not susceptible to damage a mammalian PFK. Moreover, its inhibitory effect is probably specific for this kinase because it shows no effect on two other essential kinases (HK and PyK) of the *T. brucei* glycolysis. This first irreversible selective inhibitor represents a promising lead.

The compounds that we developed in this work may assist in the crystallization of the enzyme by trapping it in a particular conformational form. Similarly, structural resolution of enzyme–inhibitor cocrystals will provide insight into the detail of interactions and thus enable the design of better and more selective inhibitory compounds, which may lead to the synthesis of new and greatly needed trypanocidal drugs.

REFERENCES

1. Périé, J., Rivière-Alric, I., Blonski, C., Gefflaut, T., Lauth de Viguerie, N., Trinquier, M., Willson, M., Oppendoes, F. R., and Callens, M. (1993) *Pharmacol. Ther.* 60, 347–365.
2. Verlinde, C. L. M. J., Haennaert, V., Blonski, C., Willson, M., Périé, J., Forthergill-Gilmore, L., Oppendoes, F. O., Gelb, M. H., Hol, W. G. J., and Michels, P. A. M. (2001) *Drug Resist. Updates* 4, 50–65.
3. Oppendoes, F. R., and Borst, P. (1977) *FEBS Lett.* 80, 360–364.
4. Bakker, B. M., Mensonides, F. I. C., Teusink, B., Van Hoek, P., Michels, P. A. M., and Westerhoff, H. V. (2000) *Proc. Natl. Acad. Sci. U.S.A.* 97, 2087–2092.
5. Michels, P. A. M., Hannaert, V., and Bringaud, F. (2000) *Parasitol. Today* 16, 482–489.
6. Oppendoes, F. R. (1987) *Annu. Rev. Microbiol.* 41, 127–151.
7. Ladame, S., Bardet, M., Périé, J., and Willson, M. (2001) *Bioorg. Med. Chem.* 9, 773–783.

8. Willson, M., Sanejouand, Y. H., Périé, J., Haennart, V., and Oppendoes, F. O. (2002) *Chem. Biol.*, in press.
9. Nwagwu, M., and Oppendoes, F. R. (1982) *Acta Tropica* 39, 61–72.
10. Cronin, C. N., and Tipton, K. F. (1985) *Biochem. J.* 227, 113–124.
11. Cronin, C. N., and Tipton, K. F. (1987) *Biochem. J.* 245, 13–18.
12. Flynn, I. W., and Bowman, I. B. R. (1980) *Arch. Biochem. Biophys.* 200, 401–409.
13. Van Schaftingen, E., Oppendoes, F. R., and Hers, H. G. (1985) *Eur. J. Biochem.* 153, 403–406.
14. Misset, O., Bos, O. J. M., and Oppendoes, F. R. (1986) *Eur. J. Biochem.* 157, 441–453.
15. Michels, P. A. M., Chevalier, N., Oppendoes, F. R., Rider, M. H., and Rigden, D. (1997) *Eur. J. Biochem.* 250, 698–704.
16. Mikaelian, I., and Sergeant, A. (1992) *Nucleic Acids Res.* 20, 376–381.
17. Blackwell, J. R., and Horgan, R. (1991) *FEBS Lett.* 295, 10–12.
18. Claustre, S., Bringaud, F., Azéma, L., Baron, R., Périé, J., and Willson, M. (1999) *Carbohydr. Res.* 315, 339–344.
19. Taguchi, Y., and Mushika, Y. (1975) *J. Org. Chem.* 40, 2310–2313.
20. Ladame, S., Claustre, S., and Willson, M. (2001) *Phosphorus, Sulfur Silicon Relat. Elem.* 174, 37–47.
21. Gelpi, J. L., Avilès, J. J., Busquets, M., Imperial, S., Mazo, A., Cortès A., Halsall, D. J., and Holbrook, J. J. (1993) *J. Chem. Educ.* 70, 805–816.
22. Lehrer, S. S. (1971) *Biochemistry* 10, 3254–3267.
23. Cleland, W. W. (1963) *Biochim. Biophys. Acta* 67, 183–187.
24. Segel, I. H. (1974) *Enzyme Kinetics*, John Wiley & Sons, New York.
25. Fromm, H. J., and Zewe, V. (1962) *J. Biol. Chem.* 237, 3027–3032.
26. Fromm, H. J. (1995) *Methods Enzymol.* 249, 123–144.
27. Burstein, E. A., Vadenkina, N. S., and Ivkova, M. N. (1974) *Photochem. Photobiol.* 18, 263–279.
28. Gryczensky, I., Wicz, W., Johnson, M. L., and Lakowicz, J. R. (1988) *Biophys. Chem.* 32, 173–185.
29. Zukin, R. S. (1979) *Biochemistry* 18, 2139–2145.
30. Shirakihara, Y., and Evans, P. R. (1988) *J. Mol. Biol.* 204, 973–994.
31. Evans, P. R., Farrants, G. W., and Hudson, P. J. (1981) *Philos. Trans. R. Soc. London B* 293, 56–62.
32. Hanson, R. L., Rudolph, F. B., and Lardy, H. A. (1973) *J. Biol. Chem.* 248, 7852–7865.
33. Bar-Tana, J., and Cleland, W. W. (1974) *J. Biol. Chem.* 249, 1263–1273.
34. Blangy, D., Buc, H., and Monod, J. (1968) *J. Mol. Biol.* 31, 13–35.
35. Deville-Bonne, D., Laine, R., and Garel, J. R. (1991) *FEBS Lett.* 290, 173–176.
36. Zheng, R. L., and Kemp, R. G. (1992) *J. Biol. Chem.* 267, 23640–23645.
37. Riquelme, P. T., Wernette-Hammond, M. E., Kneer, N. M., and Lardy, H. A. (1984) *J. Biol. Chem.* 259, 5115–5120.
38. Hellinga, H. W., and Evans, P. R. (1987) *Nature* 327, 437–439.

BI020082Z